Nicotinamide 2-Fluoroadenine Dinucleotide Unmasks the NAD^+ Glycohydrolase Activity of *Aplysia californica* Adenosine 5′-Diphosphate Ribosyl Cyclase

Bo Zhang,[‡] Hélène Muller-Steffner,[§] Francis Schuber,[§] and Barry V. L. Potter*[,‡]

Wolfson Laboratory of Medicinal Chemistry, Department of Pharmacy and Pharmacology, University of Bath, Claverton Down, Bath BA2 7AY, United Kingdom, and Département de Chimie Bioorganique, Faculté de Pharmacie, Institut Gilbert Laustriat, UMR 7175 CNRS, Université Louis Pasteur (Strasbourg I), 74 route du Rhin, 67400 Strasbourg-Illkirch, France

Received September 18, 2006; Revised Manuscript Received January 29, 2007

ABSTRACT: ADP-ribosyl cyclases catalyze the transformation of nicotinamide adenine dinucleotide (NAD^+) into the calcium-mobilizing nucleotide second messenger cyclic adenosine diphosphoribose (cADP-ribose) by adenine N1-cyclization onto the C-1″ position of NAD^+. The invertebrate *Aplysia californica* ADP-ribosyl cyclase is unusual among this family of enzymes by acting exclusively as a cyclase, whereas the other members, such as CD38 and CD157, also act as NAD^+ glycohydrolases, following a partitioning kinetic mechanism. To explore the intramolecular cyclization reaction, the novel nicotinamide 2-fluoro-adenine dinucleotide (2-fluoro-NAD^+) was designed as a sterically very close analogue to the natural substrate NAD^+, with only an electronic perturbation at the critical N1 position of the adenine base designed to impede the cyclization reaction. 2-Fluoro-NAD^+ was synthesized in high yield via Lewis acid catalyzed activation of the phosphoromorpholidate derivative of 2-fluoroadenosine 5′-monophosphate and coupling with nicotinamide 5′-monophosphate. With 2-fluoro-NAD^+ as substrate, *A. californica* ADP-ribosyl cyclase exhibited exclusively a NAD^+ glycohydrolase activity, catalyzing its hydrolytic transformation into 2-fluoro-ADP-ribose, albeit at a rate ca. 100-fold slower than for the cyclization of NAD^+ and also, in the presence of methanol, into its methanolysis product β-1″-*O*-methyl 2-fluoro-ADP-ribose with a preference for methanolysis over hydrolysis of ca. 100:1. CD38 likely converted 2-fluoro-NAD^+ exclusively into the same product. We conclude that *A. californica* ADP-ribosyl cyclase can indeed be classified as a multifunctional enzyme that also exhibits a classical NAD^+ glycohydrolase function. This alternative pathway that remains, however, kinetically cryptic when using NAD^+ as substrate can be unmasked with a dinucleotide analogue whose conversion into the cyclic derivative is blocked. 2-Fluoro-NAD^+ is therefore a useful molecular tool allowing dissection of the kinetic scheme for this enzyme.

Cyclic adenosine 5′-diphosphate ribose (cADP-ribose),[1] a metabolite of NAD^+ inducing intracellular calcium release in many cell types, was discovered by Lee and colleagues in the late 1980s (*1*). cADP-ribose is a potent calcium releasing second messenger (*2*), and its calcium-mobilizing ability is regulated independently of *myo*-inositol 1,4,5-trisphosphate (*1*, *3*), by the gating property of the ryanodine receptor, as reviewed by Guse et al. (*4*, *5*). The cyclic structure of cADP-ribose was fully established by X-ray crystallography by Lee et al. (*6*). An N-glycosidic linkage is formed between the N1 of the adenine base of NAD^+ with the anomeric carbon of the terminal ribosyl moiety by cleavage of the nicotinamide group. In biological systems, the first known enzyme converting NAD^+ (**1**) into cADP-ribose (**2**) (Figure 1) was identified as *Aplysia californica* ADP-ribosyl cyclase, a water-soluble protein that was later purified and structurally analyzed (*7*−*9*). It has been reported that *A. californica* ADP-ribosyl cyclase exhibits mainly a cyclase activity and also a cADP-ribose hydrolase activity that, however, is only markedly detectable at high enzyme concentrations (*10*). Cloning of *A. californica* ADP-ribosyl cyclase revealed a striking amino acid sequence identity with CD38, a known mammalian lymphocyte antigenic marker, that was subsequently demonstrated to be a "multifunctional" enzyme that catalyzes the transformation of NAD^+ into cADP-ribose (**2**) (ADP-ribosyl cyclase activity) and ADP-ribose (**3**) (NAD^+ glycohydrolase activity) and the solvolysis of cADP-ribose into ADP-ribose (cADPR hydrolase activity) (Figure 1) (*11*, *12*). Finally, CD38 was also found to be identical to the well-known mammalian NAD^+ glycohydrolases (*13*, *14*) that are classically known to catalyze both the hydrolysis and transglycosidation of NAD^+ and later on to be also involved in the metabolism of cADP-ribose (*12*, *15*, *16*).

CD38 transforms NAD^+ into ADP-ribose as the major product and cADP-ribose as the minor product (<2% of the total reaction products); this explains why the ADP-ribosyl

* Corresponding author. Fax: +44-1225-386114. Tel: +44-1225-386639. E-mail: B.V.L.Potter@bath.ac.uk, prsbvlp@bath.ac.uk.

‡ University of Bath.

§ Université Louis Pasteur.

[1] Abbreviations: cADP-ribose, cyclic adenosine 5′-diphosphate ribose; ADP-ribose, adenosine 5′-diphosphate ribose; NAD^+, nicotinamide adenine 5′-dinucleotide; NGD^+, nicotinamide guanine 5′-dinucleotide; NHD^+, nicotinamide hypoxanthine 5′-dinucleotide; FAB, fast atom bombardment; NMN^+, nicotinamide 5′-mononucleotide; TEP, triethyl phosphate; TEAB, triethylammonium bicarbonate; 1,N^6-etheno-NAD^+, nicotinamide 1,N^6-ethenoadenine 5′-dinucleotide; K_m, Michaelis constant.

10.1021/bi061933w CCC: $37.00
Published on Web 03/07/2007

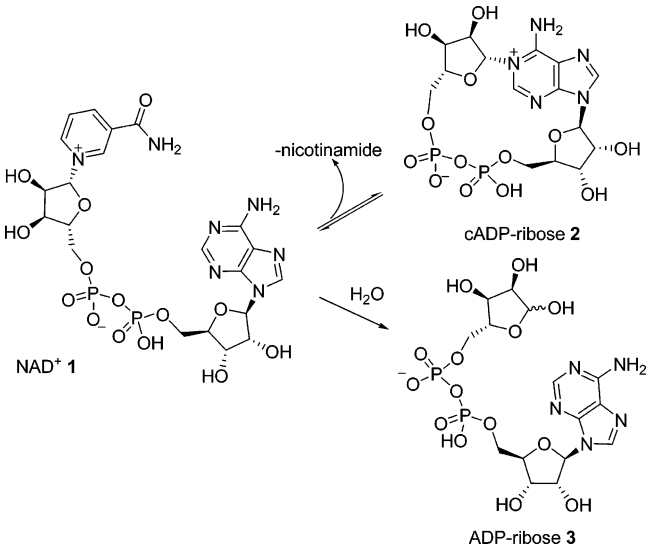

FIGURE 1: Conversion of NAD^+ into cADP-ribose and ADP-ribose.

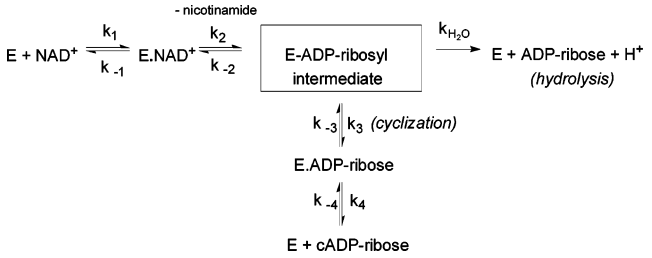

FIGURE 2: The partitioning mechanism for CD38.

cyclase activity of the "classical" mammalian NAD^+ glycohydrolases had been overlooked for so long. In contrast, the invertebrate *A. californica* ADP-ribosyl cyclase converts NAD^+ almost exclusively into the cyclic product. The limited cADP-ribose production by the multifunctional enzyme CD38 then triggered a hypothesis known as the "sequential mechanism", according to which cADP-ribose, generated from NAD^+, is quickly turned over to ADP-ribose by the cADP-ribose hydrolase function of the same enzyme. Accordingly, the "apparent" NAD^+ glycohydrolase activity of CD38 seems to result from the addition of its ADP-ribosyl cyclase and cADPR-ribose hydrolase activity (*11*). This mechanism was found to be incorrect, and a "partitioning mechanism" was subsequently proposed (Figure 2) (*17*, *18*), according to which a common enzyme−ADP-ribosyl intermediate partitions between two competing pathways: a reversible intramolecular pathway producing cyclic ADP-ribose and the macroscopically irreversible intermolecular hydrolytic pathway leading to the formation of ADP-ribose (*19*). The reversibility of the cyclization pathway coupled to the irreversibility of the solvolysis pathways explains the cADPR-ribose hydrolase activity of CD38. Altogether, according to the kinetic modeling of the partitioning mechanism, the proportion of cADP-ribose produced from NAD^+ by ADP-ribosyl cyclases is related to the relative efficiency of the cyclization vs hydrolysis steps (*20*); i.e., the low amount of cADP-ribose produced by CD38 is due to the fact that this enzyme is an inefficient cyclase.

On the basis of this partitioning mechanism, a kinetic scheme for *A. californica* ADP-ribosyl cyclase was also proposed (*10*). The cyclization pathway (k_3 step) of this enzyme has been fully studied, and in most cases, this enzyme produces cADP-ribose as a single product. The hydrolysis product ADP-ribose is kinetically highly disfavored and could only be observed under high enzyme concentrations when the *Aplysia* ADP-ribosyl cyclase is also able to hydrolyze cADP-ribose. Under these conditions, when starting with NAD^+, ADP-ribose that is formed seems to derive from its cyclic precursor (*10*). This conclusion results from the observation that the *Aplysia* cADP-ribose hydrolase catalyzed reaction is several orders of magnitude slower than the transformation of NAD^+ into cADP-ribose; i.e., the specificity ratio V_{max}/K_m is 10^4-fold higher for the NAD^+ cyclization compared to cADP-ribose hydrolysis (*10*). From these kinetic data the formation of a cADP-ribose intermediate seems inevitable during the *Aplysia* ADP-ribosyl cyclase catalyzed production of ADP-ribose from NAD^+, and this led to the proposal that the mechanism of this enzyme is macroscopically rather sequential (i.e., ADP-ribosyl cyclase followed by cADP-ribose hydrolase), which is a kinetically limiting form of the partitioning mechanism (*10*). Studies on poorly hydrolyzable pyridinium analogues of NAD^+, such as pyridine adenine dinucleotide ($PyAD^+$), provided further evidence in favor of the sequential mechanism. $PyAD^+$, which contains a scissile bond of higher energy, is thought to amplify the relative importance of the cADP-ribose hydrolase pathway by significantly slowing down the formation of the enzyme−ADP-ribosyl intermediate (k_2 step). It was found that when incubating $PyAD^+$ with *Aplysia* ADP-ribosyl cyclase, both cADP-ribose and ADP-ribose are formed, and at 10% reaction progress, the [cADP-ribose]/[ADP-ribose] ratio is found to be 2.2, which is later decreased as the reaction progresses, indicating a progressive hydrolysis of cADP-ribose (*10*). So far, it seems well established for pyridinium NAD^+ analogues to be hydrolyzed by *Aplysia* ADP-ribosyl cyclase via a sequential mechanism with cADP-ribose as the reaction intermediate. However, hydrolysis of the noncyclizable substrate β-nicotinamide 5′-mononucleotide (NMN^+) by highly purified *Aplysia* ADP-ribosyl cyclase revealed formally the existence of the hydrolysis pathway (k_{H_2O} step, Figure 2; classical NAD^+glycohydrolase activity) and indicated that the seemingly compulsory cyclic intermediate formation may not be inevitable (*10*, *21*). However, NMN^+ is very different in structure from the natural substrate NAD^+ and therefore may not be an effective substrate mimic to investigate the hydrolysis process catalyzed by *Aplysia* ADP-ribosyl cyclase. This raises the critical issue as to whether the hydrolysis pathway (k_{H_2O} step, Figure 2) can be uncovered during the transformation of NAD^+ and dinucleotide substrate analogues or is just a consequence of the combined activities of ADP-ribosyl cyclase and cADP-ribose hydrolase.

We therefore designed and synthesized 2-fluoro-NAD^+ (**4**) (Figure 3) as a noncyclizable substrate which, via the manipulation of the k_3/k_{H_2O} ratio (Figure 2), should allow investigation of the proposed hydrolysis pathway, namely the putative NAD^+ glycohydrolase activity of *Aplysia* ADP-ribosyl cyclase. As the size of the fluorine atom is comparable with that of a proton, 2-fluoro-NAD^+ is sterically the closest conceivable analogue of NAD^+, the natural substrate of *Aplysia* ADP-ribosyl cyclase, without any steric perturbation, and since the intramolecular cyclization of this compound at N1 should be profoundly impeded by the strong electronegativity of fluorine, 2-fluoro-NAD^+ is therefore an

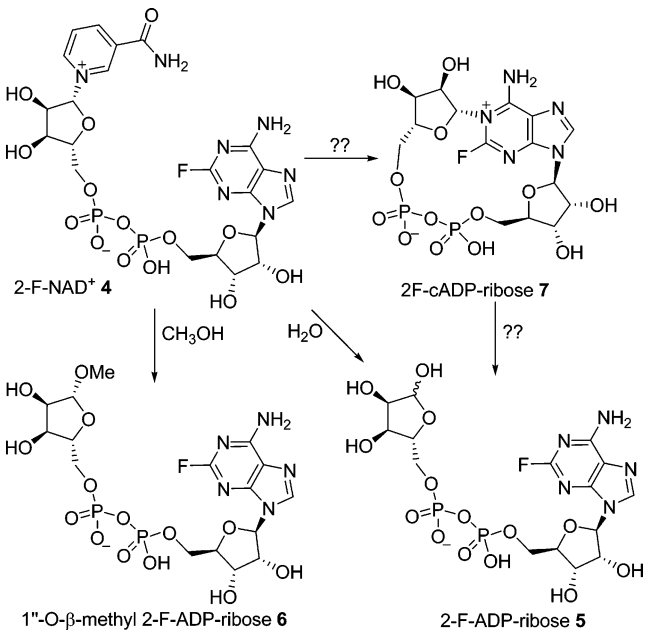

FIGURE 3: Pathways for chemical and enzymatic processing of the substrate analogue 2-fluoro-NAD^+.

ideal molecular tool to investigate the hidden hydrolysis activity of *Aplysia* ADP-ribosyl cyclase. 2-Fluoro-NAD^+ may also inhibit *Aplysia* ADP-ribosyl cyclase by forming a stable appropriately folded intermediate in the active site. We report here a synthetic route to 2-fluoro-NAD^+ and an enzymological study of its interaction with *Aplysia* ADP-ribosyl cyclase.

EXPERIMENTAL PROCEDURES

General. All reagents and solvents were of commercial quality and were used without any further purification unless described otherwise. *A. californica* ADP-ribosyl cyclase and the nucleotide pyrophosphatase obtained from *Crotalus atrox* venom were purchased from Sigma-Aldrich Co. Ltd., Gillingham, England. Highly purified ADP-ribosyl cyclase was isolated from *A. californica* as described (*10*). H_2O was of MilliQ grade. $MnCl_4$/formamide solution was dried over molecular sieves (4 Å) for 4 days before usage. All ^1H, ^{13}C, and ^{31}P NMR spectra were collected either on a JEOL Delta machine at 270 MHz (proton), 68 MHz (carbon), or 109 MHz (phosphorus) or on a Varian Mercury-Vx NMR system at 400 MHz (proton) and 100 MHz (carbon). Chemical shift values (δ) are given in parts per million (ppm). Abbreviations of the coupling patterns are as follows: br s, broad singlet; s, singlet; d, doublet; t, triplet; m, multiplet etc. UV spectra were collected on a Perkin-Elmer lambda EZ 201 or lambda 3B spectrophotometer. FAB mass spectra were recorded on samples in *m*-nitrobenzyl alcohol matrix with PEG-H/PEG monomethyl ether as reference substance for accurate mass measurements on a Microsmass Autospec instrument. All nucleotide compounds were purified on a Pharmacia Biotech Gradifrac system equipped with a peristaltic P-1 pump and a fixed wavelength UV-1 optical unit (280 nm). The following chromatography conditions were employed: ion-pair system, stationary phase, Q-Sepharose washed with MilliQ water; gradient, 1 M TEAB buffer (pH 7.1−7.6) against H_2O (0−50%); flow rate, 5 mL/min; RP system, stationary phase, LiChroprep RP-18 saturated with 0.05 M TEAB buffer; gradient, 0.05 M TEAB buffer against acetonitrile (0−30%); flow rate, 5 mL/min. HPLC analysis (system A) was carried out on a Waters 2695 Alliance module equipped with a Waters 2996 photodiode array detector (210−350 nm). A Phenomenex Synergi 4u MAX-RP 80A column (150 × 4.6 mm) and Hichrom guard column were used as the stationary phase, and the ion-pair buffer [45% phosphate buffer (pH 6.4) in MeOH and 0.17% (m/v) cetrimide] was adopted as the mobile phase. Kinetic analysis (HPLC system B) was performed either on a 300 × 3.9 mm μBondapak C_{18} column (Waters Associates, Milford, MA) or on a 250 × 4.6 mm Acclaim C_{18} (Dionex) column. The compounds were eluted isocratically at a flow rate of 1 mL/min with a 10 mM ammonium phosphate buffer, pH 5.5, containing 0.8% (v/v) acetonitrile and detected by absorbance recordings at 260 nm.

Molecular Modeling. Adenosine and 2-fluoroadenosine were minimized using the DFT (density functional theory) method with the 6-31G** basis set as implemented in the CAChe software package from Fujitsu (CAChe Version 4.4, 2000 Fujitsu Limited). As a part of the calculation the electron density surface was calculated; this was then displayed on the final minimized geometry of the molecule.

Enzyme Kinetics. The ADP-ribosyl cyclase catalyzed transformation of 2-fluoro-NAD^+ was measured by incubation at 37 °C in a 10 mM potassium phosphate buffer, pH 7.4 (200 μL final volume), in the presence of the substrate (5−500 μM) and purified enzyme (15 milliunits). At selected times, aliquots (50 μL) were removed, and the reaction was stopped by addition of ice-cold perchloric acid (2% final concentration). After neutralization with 3.5 M K_2CO_3, the precipitated proteins were removed by centrifugation. Product formation was analyzed by HPLC (system B). Kinetic parameters were determined from the plot of the initial rates as a function of substrate concentrations (eight data points) using a nonlinear regression program (GraphPad Prism).

Reaction Product Treatment with Nucleotide Pyrophosphatase. The product obtained by ADP-ribosyl cyclase catalyzed transformation of 2-fluoro-NAD^+ was further incubated at 37 °C for 10 min in the presence of nucleotide pyrophosphatase (≈50 milliunits) and analyzed by HPLC (system B).

Methanolysis of 2-Fluoro-NAD^+. 2-Fluoro-NAD^+ (200 and 300 μM) was incubated at 37 °C in a 10 mM potassium phosphate buffer, pH 7.4 (200 μL final volume), in the presence of methanol (2 and 3 M) and 15 milliunits of highly purified *Aplysia* cyclase. At different time points, aliquots were analyzed by HPLC (system B) as previously described.

*Chemical Synthesis. (A) Adenosine 5′-Diphosphate Ribose [ADP-Ribose (**3**)].* A solution of cADP-ribose (0.5 μmol) in MilliQ water (1 mL) was heated at 70 °C until HPLC analysis indicated that all of the starting cADP-ribose was consumed, and a single new peak was obtained at 10.0 min. After removal of the solvent, ADP-ribose was obtained in quantitative yield and was used as a HPLC standard without further purification: HPLC (system A) at 254 nm, 10.0 min (single peak); ^1H NMR (D_2O, 270 MHz) δ 8.57 (s, 1H, H-8 or H-2), 8.35 (s, 1H, H-2 or H-8), 6.10 (d, $J_{1',2'} = 5.4$ Hz, 1H, H-1′), 5.31 (d, $J_{1'',2''} = 4.1$ Hz, 1/3H, H-1″$_\beta$), 5.17 (m, 2/3H, H-1″$_\alpha$), 4.72−3.97 (m, 10H, ribose-H); ^{31}P NMR (D_2O, 109 MHz, ^1H decoupled) δ −10.52 (br s, 5′-P-P).

*(B) 2-Fluoroadenosine (**11**).* 2-Fluoroadenosine was synthesized according to a published protocol (*22*). 2-NH_2-adenosine (350 mg, 1.24 mmol) was dissolved in HF/pyridine (1 mL, 70%) and dry pyridine (0.2 mL). The resulting dark yellow solution was then cooled to ca. −10 °C using an ice−salt bath, and an aqueous solution of KNO_2 (0.1 mL, 1.67 g/mL) was added dropwise over 1 h. The resulting light orange suspension was stirred at ca. −6 to −8 °C for 1 h and at 3 °C for an additional 1 h. The reaction mixture was then poured into an ice-cold $CaCO_3$ slurry (2 g in 4 mL of H_2O). After the mixture was stirred at 3 °C for 2 h and room temperature overnight, the $CaF/CaCO_3$ was filtered off and washed with H_2O (3 mL) and H_2O/EtOH (4 mL, 1:1). TLC (*n*-BuOH−H_2O−acetic acid) of the filtrate showed that all of the starting 2-aminoadenosine had reacted, and a main new spot was produced at R_f 0.68, which was identical to that of the literature (*22*). The crude product was purified by column chromatography, eluted with EtOAc−MeOH−H_2O (10:2:1) or a gradient of 5−25% MeOH against DCM to give the title compound (190 mg, 54%): mp 236−240 °C [lit. (*23*), 200 °C]; ^{1}H NMR (DMSO-d_6, 400 MHz) δ 8.36 (s, 1H, H-8), 7.90 (br s, 2H, NH_2), 5.78 (d, $J_{1',2'}$ = 5.9 Hz, 1H, H-1′), 5.51 (d, $J_{2',OH}$ = 5.9 Hz, 1H, 2′-OH), 5.25 (d, $J_{3',OH}$ = 5.1 Hz, 1H, 3′-OH), 5.09 (apparent t, $J_{5'a,OH}$ = $J_{5'b,OH}$ = 5.5 Hz, 1H, 5′-OH), 4.52 (dt, $J_{2',1'}$ = $J_{2',OH}$ = 5.9 Hz and $J_{2',3'}$ = 5.1 Hz, 1H, H-2′), 4.13 (m, 1H, H-3′), 3.92 (apparent q, $J_{4',5'a}$ = $J_{4',5'b}$ = $J_{4',3'}$ = 3.9 Hz, 1H, H-4′), and 3.60 (m, 2H, H-5′); ^{1}H NMR (DMSO-d_6, 400 MHz, D_2O shake) δ 8.35 (s, 1H, H-8), 5.80 (d, $J_{1',2'}$ = 5.9 Hz, 1H, H-1′), 4.53 (dd, $J_{2',1'}$ = 5.9 Hz and $J_{2',3'}$ = 5.1 Hz, 1H, H-2′), 4.15 (dd, $J_{3',2'}$ = 5.1 Hz and $J_{3',4'}$ = 3.5 Hz, 1H, H-3′), 3.95 (apparent q, $J_{4',5'a}$ = $J_{4',5'b}$ = $J_{4',3'}$ = 3.9 Hz, 1H, H-4′), 3.67 (dd, $J_{5'a,5'b}$ = 12.1 Hz and $J_{5'a,4'}$ = 3.9 Hz, 1H, H-5′a), and 3.57 (dd, $J_{5'b,5'a}$ = 12.1 Hz and $J_{5'b,4'}$ = 3.9 Hz, 1H, H-5′b); ^{13}C NMR (DMSO-d_6, 100 MHz) δ 158.9 (d, $J_{C,F}$ = 203.7 Hz, C-2), 157.8 (d, $J_{C,F}$ = 22.0 Hz, C-6), 150.9 (d, $J_{C,F}$ = 20.6 Hz, C-4), 140.5 (C-8), 117.8 (C-5), 87.9 (C-1′), 86.0 (C-4′), 73.9 (C-2′), 70.7 (C-3′), and 61.7 (C-5′); ^{19}F NMR (DMSO-d_6, 376 MHz) δ −52.09 (s, 2-F); *m/z* (FAB^+) 286.2 [$(M + H)^+$, 20%].

*(C) 2-Fluoroadenosine 5′-Monophosphate (**12**).* 2-Fluoroadenosine (250 mg, 0.88 mmol) was dissolved in TEP (2.5 mL) by heating with a heat gun. It was then cooled to 0 °C. H_2O (0.01 mL) was added followed by $POCl_3$ (0.45 mL, 4.83 mmol), and the reaction mixture was stirred at 0 °C for a further 4 h after which HPLC analysis showed that more than 80% of starting material was consumed. Excess $POCl_3$ was then removed under vacuum, H_2O (10 mL) was added at 0 °C, and the mixture was stirred for 1 h. TEP was removed by partition between water and ice-cold ethyl acetate (3 × 10 mL). The aqueous layer was concentrated under vacuum, and the resulting white residue was redissolved in 0.1% aqueous LiOH (15 mL). Crude 2-fluoro-AMP lithium salt was precipitated in acetone (200 mL) and then purified by reverse-phase chromatography, eluted with a gradient of 0−30% MeCN in 0.05 M TEAB buffer. The appropriate fractions were collected and evaporated under reduced pressure. The residue obtained was dissolved in H_2O (10 mL) and treated with charcoal (2 spoons) for 1 h to remove any residual inorganic phosphate. Elution with EtOH−H_2O−NH_3 (400 mL, 25:24:1) provided the 2-fluoro-AMP ammonium salt which was further treated with DOWEX-H^+ to give the desired 2-fluoro-AMP as its free acid (160 mg, 50%): HPLC (system A) at 254 nm, 7.80 min (single peak); ^{1}H NMR (D_2O, 400 MHz) δ 8.85 (s, 1H, H-8), 6.00 (d, $J_{1',2'}$ = 5.4 Hz, 1H, H-1′), 4.61 (m, 1H, H-2′), 4.33 (m, 1H, H-3′), 4.13 (m, 1H, H-4′), and 4.01 (m, 2H, H-5′); ^{13}C NMR (D_2O, 68 MHz) δ 159.6 (d, $J_{C,F}$ = 212.6 Hz, C-2), 155.5 (d, $J_{C,F}$ = 20.5 Hz, C-6), 149.4 (d, $J_{C,F}$ = 21.0 Hz, C-4), 138.8 (C-8), 112.9 (C-5), 89.4 (C-1′), 83.7 (d, $J_{C,P}$ = 8.3 Hz, C-4′), 74.6 (C-2′), 69.5 (C-3′), and 64.3 (d, $J_{C,P}$ = 5.4 Hz, C-5′); ^{31}P NMR (D_2O, 109 MHz, ^{1}H decoupled) δ 0.68 (s, 5′-P); ^{19}F NMR (D_2O, 376 MHz) δ −52.70 (s, 2-F); *m/z* (FAB^-) 364.0 [$(M - H)^-$, 100%]; HRMS (FAB^-) calcd for $C_{10}H_{12}N_5FO_7P^-$ $(M - H)^-$, 364.0464; found 364.0464.

*(D) 2-Fluoroadenosine 5′-Monophosphate Morpholidate (**13**).* 2-Fluoro-AMP free acid (160 mg, 0.44 mmol) was dissolved in dry DMSO (0.9 mL) and coevaporated with dry DMF (3 × 2 mL). The resulting yellow residue was dissolved in DMSO (1 mL), and dipyridyl disulfide (300 mg, 1.36 mmol), morpholine (0.3 mL, 3.43 mmol), and triphenylphosphine (300 mg, 1.15 mmol) were added in sequence. The reaction mixture was stirred at room temperature for 3 h after which ^{31}P NMR showed completion of the reaction [disappearance of the monophosphate peak and formation of a new singlet at ca. 5.7 ppm (DMSO) for the morpholidate]. Precipitation of the product occurred by dropwise addition of a solution of NaI in acetone (20 mL), and the resulting precipitate was filtered and washed with acetone to yield the desired morpholidate as a yellow solid (159 mg, 84%): HPLC (system A) at 254 nm, 3.67 min (single peak); ^{1}H NMR (D_2O, 270 MHz) δ 8.31 (s, 1H, H-8), 5.93 (d, $J_{1',2'}$ = 5.4 Hz, 1H, H-1′), 4.73 (apparent t, $J_{2',1'}$ = $J_{2',3'}$ = 5.4 Hz, 1H, H-2′), 4.47 (dd, $J_{3',2'}$ = 5.4 Hz and $J_{3',4'}$ = 3.5 Hz, 1H, H-3′), 4.30 (m, 1H, H-4′), 3.98 (m, 2H, H-5′), 3.54 (m, 4H, $2CH_2O$), and 2.90 (m, 4H, $2CH_2N$); ^{13}C NMR (D_2O, 68 MHz) δ 159.0 (d, $J_{C,F}$ = 210.6 Hz, C-2), 157.2 (d, $J_{C,F}$ = 22.0 Hz, C-6), 150.2 (d, $J_{C,F}$ = 22.0 Hz, C-4), 139.8 (C-8), 117.1 (C-5), 87.5 (C-1′), 83.7 (d, $J_{C,P}$ = 8.2 Hz, C-4′), 74.1 (C-2′), 70.3 (C-3′), 67.0, 66.9 (both CH_2O), 63.9 (d, $J_{C,P}$ = 5.4 Hz, C-5′), 44.7 ($2CH_2N$); ^{31}P NMR (D_2O, 109 MHz, ^{1}H decoupled) δ 8.16 (s, 5′-P); ^{19}F NMR (D_2O, 376 MHz) δ −52.81 (2-F); *m/z* (FAB^-) 433.0 [$(M - H)^-$, 100%]; HRMS (FAB^-) calcd for $C_{14}H_{19}FN_6O_7P^-$ $(M - H)^-$, 433.1042; found 433.1021.

*(E) Nicotinamide 2-Fluoroadenine Dinucleotide (**4**).* To a solution of 2-fluoro-AMP morpholidate (25 mg, 58 μmol) in $MnCl_2$/formamide (0.56 mL, 0.2 M) was added β-NMN^+ (25 mg, 75 μmol) and $MgSO_4$ (17 mg, 140 μmol) under an argon atmosphere. The resulting suspension was stirred at room temperature for 48 h after which HPLC analysis showed completion of the reaction with formation of a new peak at 3.70 min. Precipitation of the product occurred by addition of MeCN (3 mL). It was filtered, dissolved in MilliQ water (2 mL), and treated with Chelex−Na^+ to remove any residual Mn^+ and then purified on a reverse-phase system, eluted with 0−30% MeCN against 0.05 M TEAB buffer. The appropriate fractions were combined and evaporated under reduced pressure, and the excess TEAB was destroyed by coevaporation with methanol to give 2-F NAD^+ (32 μmol, 55%) as its triethylaminium salt: HPLC (system A) at 254 nm, 3.70 min (single peak); UV (H_2O) λ_{max} 262 nm (ϵ/dm^3 mol^{-1} cm^{-1} 16308); ^{1}H NMR (D_2O, 270 MHz)

Scheme 1[a]

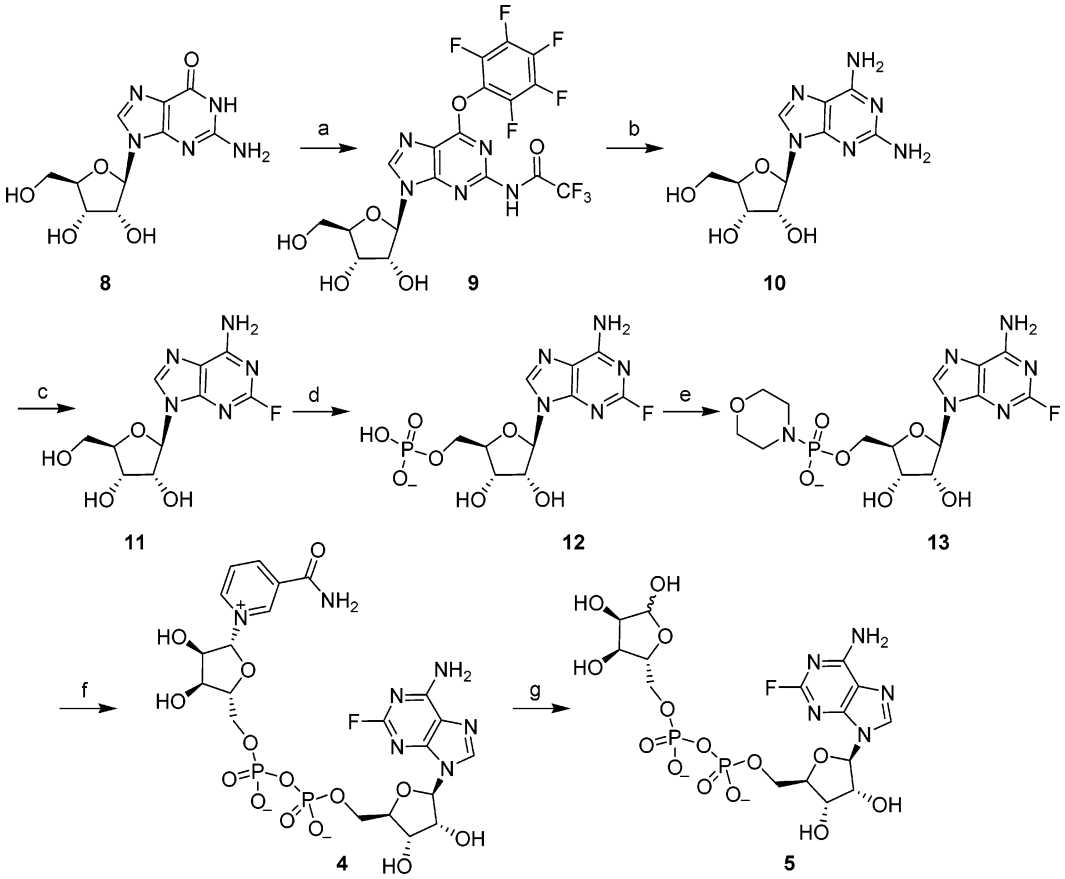

[a] Reagents and conditions: (a) i-TFAA, pyridine, 0 °C, 15 min; ii-pentafluorophenol, room temperature, 79%; (b) saturated ammonia aqueous solution, 55 °C, 60%; (c) HF/pyridine 56%, KNO_2 54%; (d) TEP, $POCl_3$, H_2O, 0 °C, 50%; (e) PPh_3, dipyridyl disulfide, morpholine, room temperature, 84%; (f) $MnCl_2$/formamide, $MgSO_4$, β-NMN^+, room temperature, 55%; (g) 25 mM pH 7.4 HEPES buffer, ADP-ribosyl cyclase, 70%.

δ 9.34 (s, 1H, H_N-2), 9.17 (d, $J_{6,5} = 6.2$ Hz, 1H, H_N-6), 8.86 (d, $J_{4,5} = 8.1$ Hz, 1H, H_N-4), 8.33 (s, 1H, H-8), 8.22 (dd, $J_{5,4} = 8.1$ Hz and $J_{5,6} = 6.2$ Hz, 1H, H_N-5), 6.08 (d, $J_{1'',2''} = 5.7$ Hz, 1H, H-1″), 5.89 (d, $J_{1',2'} = 5.9$ Hz, 1H, H-1′), 4.78 (m, 1H, H-2′), 4.52−4.20 (m, 9H, ribose-H); ^{13}C NMR (D_2O, 100 MHz) δ 165.1 (CO), 158.7 (d, $J_{C,F} = 211.6$ Hz, C-2), 156.7 (d, $J_{C,F} = 22.0$ Hz, C-6), 150.3 (C-4), 145.7 (C_N4), 142.4 (C_N6), 139.8 (C-8, C_N2), 134.6 (C_N3), 128.6 (C_N5), 118.2 (C-5), 99.9 (C-1″), 87.0 (C-1′), 86.7 (C-4′), 83.7 (C-4″), 77.5 (C-2″), 73.9 (C-2′), 70.6 (C-3″), 70.2 (C-3′), 65.3 (C-5″), 64.9 (C-5′); ^{31}P NMR (D_2O, 109 MHz, ^{1}H decoupled) δ −10.77 (m, 5′-P-P); ^{19}F NMR (D_2O, 376 MHz) δ −52.73 (s, 2-F); *m*/*z* (FAB^-) 681.0 [$(M)^-$, 100%]; HRMS (FAB^-) calcd for $C_{21}H_{26}FN_7O_{14}P_2^-$ $(M)^-$, 681.0997; found 681.0975.

*(F) 2-Fluoroadenosine Diphosphate Ribose (**5**).* 2-Fluoro-NAD^+ (61 μmol) was incubated with *A. californica* ADP-ribosyl cyclase (200 μL) in a 25 mM HEPES buffer (pH 7.4, 110 mL) at room temperature. After 48 h, HPLC analysis indicated that all starting 2-fluoro-NAD^+ was consumed. The crude reaction solution was diluted with MilliQ water until the conductivity was reduced to less than 200 μS/cm and product was purified by ion-exchange chromatography, eluting with a 0−50% gradient of 1 M TEAB against MilliQ water. The appropriate fractions were collected and concentrated under reduced pressure. Excess TEAB was removed by coevaporating with methanol to give the hydrolyzed product 2-F-ADP-ribose (**5**) (43 μmol, 70%) as a glassy solid: HPLC (system A) at 254 nm, 10.51 min (single peak); UV (H_2O) λ_{max} 262 nm (ϵ/dm^3 mol^{-1} cm^{-1} 13759); ^{1}H NMR (D_2O, 400 MHz) δ 8.28 (1H, s, H-8), 5.85 (d, $J_{1',2'} = 5.9$ Hz, 1H, H-1′), 5.18 (d, $J_{1'',2''} = 2.4$ Hz, 1/3H, H-1″$_\beta$), 5.06 (d, $J_{1'',2''} = 4.4$ Hz, 2/3H, H-1″$_\alpha$), 4.59 (dd, $J_{2',1'} = 5.9$ Hz and $J_{2',3'} = 5.4$ Hz, 1H, H-2′), 4.38 (m, 1H, H-3′), 4.24 (m, 1H, H-4′), 4.15−3.86 (m, 7H, ribose-H); ^{31}P NMR (D_2O, 109 MHz, ^{1}H decoupled) δ −10.39 (d, $J_{P,P} = 18.2$ Hz), −10.82 (d, $J_{P,P} = 18.2$ Hz); ^{19}F NMR (D_2O, 376 MHz) δ −53.94, −53.98 (α, β mixture); *m*/*z* (FAB^-) 575.9 [$(M - H)^-$, 60%]; HRMS (FAB^-) calcd for $C_{15}H_{21}FN_5O_{14}P_2^-$ $(M - H)^-$, 576.0550; found 576.0556.

RESULTS AND DISCUSSION

Synthesis of 2-Fluoro-NAD$^+$. 2-Fluoro-NAD^+ was synthesized by an adaptation of a previous synthesis of NAD^+ by Lee et al. (*24*), and the key nucleoside building block 2-fluoroadenosine was synthesized from guanosine (**8**) (Scheme 1). Treatment of guanosine with trifluoroacetic acid anhydride followed by addition of pentafluorophenol activates the C-6 position by forming a good leaving group (*25*). Compound **9** was produced in 79% yield as an oil that was then heated in concentrated aqueous ammonia solution, giving 2-aminoadenosine (**10**) in 60% yield (*26*). The crucial fluorine atom was introduced at the C-2 position via a Schiemann reaction (*22*). The 2-fluoroadenosine structure (**11**) was confirmed on the basis of the following evidence: in the ^{1}H NMR spectrum we observed the disappearance of the 2-NH_2 peak, which normally has a chemical shift at

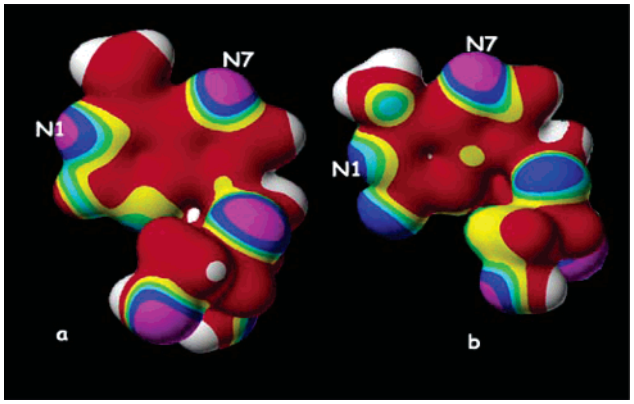

FIGURE 4: Computer modeling results for adenosine (a) and 2-fluoroadenosine (b). Values at the color boundaries (partial charge): white, 0.090; red, 0.030; yellow, 0.010; green, 0.000; light blue, −0.010; dark blue, −0.030; pink, −0.060.

5−6 ppm and integration of two protons; in the ^{19}F NMR spectrum a singlet appeared at −53 ppm, suggesting the occurrence of fluorine substitution; and in the ^{13}C NMR spectrum the coupling constant ($J_{C,F}$) between 2-F and C-2 was ca. 200 Hz, which was in agreement with the reported fluorine carbon coupling constant for trifluoroacetic acid (*27*). This structure was further confirmed by mass spectrometry where a three mass unit increase compared to 2-aminoadenosine was observed. Phosphorylation of 2-fluoroadenosine (**11**) was accomplished using the TEP/$POCl_3$ method reported by Ikemoto et al. (*28*). The 2-fluoro-5′-AMP (**12**) was transformed to its lithium salt before purification as, according to our observation, the lithium salt had a better separation from the inorganic phosphate than the sodium salt on a reverse-phase medium. The crude 2-fluoro-5′-AMP was purified on an RP-18 column and was then treated with charcoal to remove any excess inorganic phosphate. Prior to coupling with β-NMN$^+$, the monophosphate 2-fluoro-5′-AMP (**12**) was activated through a triphenylphosphine/dipyridyl disulfide-mediated condensation with morpholine. Starting from 2-fluoro-5′-AMP free acid, this activation reaction was completed in 3 h in more than 80% yield. As suggested by the mechanism proposed by Mukaiyama et al. (*29*), the free acid is the appropriate starting material in the formation of the morpholidate. However, we observed that this reaction could also proceed using the triethylammonium salt without affecting the reaction rate and yield. ^{31}P NMR spectroscopy was employed to monitor the formation of the morpholidate (**13**), where a new singlet at 5.7 ppm (DMSO-d_6) or at 8.1 ppm (D_2O) is normally expected (*30*). Coupling of 2-fluoro-AMP morpholidate and β-NMN$^+$ was accomplished in $MnCl_4$/formamide solution in the presence of dry $MgSO_4$. The novel 2-fluoro-NAD$^+$ (**4**) was produced and isolated by reverse-phase chromatography in 55% yield as its triethylammonium salt. Compound (**4**) was quantified using total phosphate analysis, and the extinction coefficient of this compound was also determined.

Molecular Modeling. 2-Fluoro-NAD$^+$, as a noncyclizable NAD$^+$ analogue, was explored by computer modeling using the CAChe software package (Figure 4). Partial charges on the N1 position of the nucleosides 2-fluoroadenosine and adenosine were calculated and compared in this study, and the expected decrease in electron density at the N1 position of 2-fluoroadenosine was explored relative to the unsubstituted nucleobase (Figure 4). Note the pink (−0.060) to dark blue (−0.030) transformation at N1 in adenosine and 2-fluoroadenosine, respectively. We thus assumed that the N1 electron density of the complete dinucleotide 2-fluoro-NAD$^+$ is also decreased compared with that of NAD$^+$. Since the electron density of N1 is reduced and since electron density parallels nucleophicility, the attack of the N1 on the nicotinamide-bearing ribose at C-1″ of 2-fluoro-NAD$^+$ should be blocked, and therefore the cyclization catalyzed by ADP-ribosyl cyclase at the N1 position of 2-fluoro-NAD$^+$ is most unlikely to proceed.

Another important line of evidence for 2-fluoro-NAD$^+$ not being cyclizable comes from the work of Fischer et al. (*31*). In their studies on a different, but related, system they experimentally calculated the pK_a value of N1 of 2-modified adenosine 5′-triphosphate using ^{15}N NMR measurements. ^{15}N NMR is a tool to study the basicity of the nucleotide base in an unambiguous fashion (*32*), and because ^{15}N NMR spectra are measured in H_2O, it can provide pK_a values that are of biological relevance. With an electron-withdrawing group attached at the 2 position in ATP, the pK_a value decreased dramatically. The experimental pK_a value at N1 for 2-chloro-ATP is −0.2, and compared to that of ATP (pK_a 4.16), the value decreases strikingly by some 4 log units. NAD$^+$ shares the same adenine base moiety as ATP, and since we know that fluorine has a stronger electron-withdrawing effect than chlorine, the pK_a of 2-fluoro-NAD$^+$ should therefore be still further decreased. A nitrogen atom of such an apparently low pK_a will not be likely to accomplish the nucleophilic attack on the ribose C-1″ of the enzyme−ADP-ribosyl intermediate as low basicity parallels low nucleophilicity. This is then compelling evidence that allows us to rule out the intermediacy of a 2-fluoro-cADP-ribose species as a potential product after incubation of 2-fluoro-NAD$^+$ with the cyclase. 2-Fluoro-NAD$^+$ may therefore be an ADP-ribosyl cyclase inhibitor and/or a new tool to study the enzyme−substrate interaction mechanism.

Enzymology and Kinetics. In order to study the enzymatic reactions of 2-fluoro-NAD$^+$, compound (**4**) was first incubated with commercially available invertebrate *Aplysia* ADP-ribosyl cyclase at room temperature. A single product was seen in this reaction which was the hydrolysis product 2-fluoro-ADP-ribose (**5**) (Figure 3), thus uncovering an NAD$^+$ glycohydrolase activity of the *Aplysia* cyclase. Three lines of evidence suggested that the reaction product was 2-fluoro-ADP-ribose. First, the ^{1}H NMR pattern observed for this compound was clearly identical to that of standard ADP-ribose (NMR of ADP-ribose; see Experimental Procedures). Two sets of doublets at 5.3 and 5.1 ppm that integrated as 1/3 proton and 2/3 protons, respectively, indicated that both the α-hydroxyl and the β-hydroxyl group were produced at the anomeric carbon of the terminal ribose derived from the nicotinamide end. Second, the elution time of 2-fluoro-ADP-ribose in an ion-pair HPLC system (system A; for details see Experimental Procedures) is ca. 10.5 min, which is close to that of the ADP-ribose standard (10.0 min). Third, mass spectrometry of the 2-fluoro-ADP-ribose product showed a major positive ion of 576 mass units, which is 17 mass units greater than that calculated for the 2-fluoro-cADP-ribose, consistent with the hydrolyzed form. Because it was crucial to control for the potential activity of a contaminating glycohydrolase in the commercial enzyme, we thus undertook

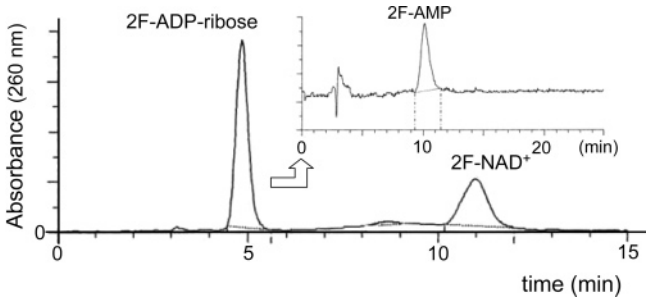

FIGURE 5: Hydrolysis of 2-fluoro-NAD$^+$ by highly purified *Aplysia* ADP-ribosyl cyclase. HPLC analysis indicates that 2-fluoro-NAD$^+$ was transformed into 2-fluoro-ADP-ribose. The 2-fluoro-ADP-ribose peak was collected and hydrolyzed into 2-fluoro-5′-AMP with nucleotide pyrophosphatase. Inset: HPLC profile of the hydrolysis reaction.

Table 1: Kinetic Constants of Substrate Transformation Catalyzed by *A. californica* ADP-Ribosyl Cyclase at pH 7.4

substrate	K_m (μM)	V_{max} (μmol min^{-1} mg^{-1})	K^a
NAD$^{+\,b}$	4.6 ± 0.4	465 ± 57	
cADP-ribose^b	1040 ± 150	3.34 ± 1.15	152
2-fluoro-NAD$^+$	16.05 ± 3.36	15.47 ± 0.69	100

^{a} Methanol/water partitioning ratio of the reaction intermediate. ^{b} NAD$^+$ and cADP-ribose were transformed respectively into cADP-ribose and ADP-ribose; data from ref *10*.

a full enzyme kinetic study using a highly purified *A. californica* cyclase (10).

HPLC (system B; see Experimental Procedures) analysis of the transformation of 2-fluoro-NAD$^+$ (11.0 min), catalyzed by this highly purified cyclase, indicated that during the whole reaction course only a single product was formed that had an elution time very similar to that of ADP-ribose (4.9 min, Figure 5). The same reaction product was also obtained by hydrolysis of 2-fluoro-NAD$^+$ catalyzed by recombinant human CD38 (data not shown), which acts predominantly as a NAD$^+$ glycohydrolase rather than a cyclase. This product, when incubated in the presence of a nucleotide pyrophosphatase, was also totally transformed into a compound that had an elution time similar to that of 5′-AMP (Figure 5). These experiments indicated that, by analogy with CD38, *A. californica* ADP-ribosyl cyclase did hydrolyze the 2-fluoro-NAD$^+$ into 2-fluoro-ADP-ribose (**5**) without forming 2-fluoro-cADP-ribose (**7**) or any other cyclic intermediates. Within the limits of our analytical methods no cyclization was observed (i.e., <1% reaction products), and it was not practical to pursue the unlikely possibility of such small amounts of cyclic product being formed. This applies also equally to the possibility of putative N7 cyclization to give (**14**) (Figure 9).

Kinetic parameters determined for the *Aplysia* cyclase catalyzed 2-fluoro-NAD$^+$ hydrolysis reaction were K_m = 16.05 ± 3.36 μM and V_{max} = 15.47 ± 0.69 μmol·min^{-1}·mg^{-1}. Compared to the V_{max} of NAD$^+$ cyclization, the *A. californica* ADP-ribosyl cyclase catalyzed hydrolysis of 2-fluoro-NAD$^+$ is about 2 orders of magnitude slower (Table 1). This is an interesting observation because a major difference in the activation energy of the nicotinamide−ribose bond cleavage (k_2 step) is not expected between NAD$^+$ and its analogue; consequently, the rate difference found for their catalyzed transformation, respectively into cADP-ribose and 2-fluoro-ADP-ribose, confirms the fact that the hydrolytic pathway

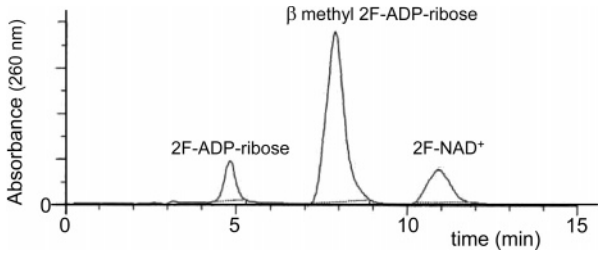

FIGURE 6: Methanolysis of 2-fluoro-NAD$^+$ by highly purified *Aplysia* ADP-ribosyl cyclase.

(k_{H_2O} step) is a slow step, relative to the formation of the reaction intermediate, in the kinetic mechanism of the *Aplysia* ADP-ribosyl cyclase. The K_m for the unnatural substrate is a little higher than that for NAD$^+$ (K_m = 4.6 ± 0.4 μM).

A. californica ADP-ribosyl cyclase was found previously to also catalyze the methanolysis of cADP-ribose, and on a molar basis, the rate of this reaction was reported to be about 150-fold faster than that of its hydrolysis reaction (*10*). In order to further rationalize the partitioning mechanism and to reveal the cryptic NAD$^+$ glycohydrolase activity of the cyclase, the enzyme-mediated methanolysis of 2-fluoro-NAD$^+$ was also studied. Under the experimental conditions used, a new product was formed when 2-fluoro-NAD$^+$ was incubated with the cyclase in the presence of methanol. On HPLC (system B; see Experimental Procedures), the elution time of this newly formed product at 7.9 min (Figure 6) corresponds to what would be expected for the β-1″-*O*-methyl 2-fluoro-ADP-ribose (**6**) (structure in Figure 3). This observation clearly indicates the existence of the NAD$^+$ methanolysis activity of *Aplysia* ADP-ribosyl cyclase, since formation of 2-fluoro-cADP-ribose is highly unlikely in this case and the methanolysis product could only be formed directly from 2-fluoro-NAD$^+$ via the NAD$^+$ glycohydrolase activity.

The ratios between methanolysis and hydrolysis products were also found to be proportional to the methanol concentration (0−3 M; not shown). We estimated the relative efficacy of water and methanol in the nucleophilic attack of the E−ADP-ribosyl intermediate by calculating the partitioning ratio using the equation:

$$K = [\beta\text{-methyl 2-F-ADP-ribose}][H_2O]/[\text{2-F-ADP-ribose}][\text{methanol}]$$

The ratio *K* was found to be around 100 (Table 1), which is in agreement with the fact that methanol is a better acceptor than water in this type of reaction (*33*). Importantly, in the presence of 3 M methanol which greatly increases the turnover rate of the E−ADP-ribosyl intermediate, the overall rate of 2-fluoro-NAD$^+$ transformation was also affected. The observed doubling of the initial rate (not shown) indicates, in agreement with the finding on the V_{max} (see above), that for the catalytic transformation of this substrate, the k_{H_2O} step is part of the rate-limiting step. It appears, therefore, that 2-fluoro-NAD$^+$ is a molecular tool which allows dissection of the kinetic scheme (Figures 2 and 7), and its solvolysis data confirm that, in contrast to CD38, in the *Aplysia* cyclase-catalyzed reactions the capture of the E−ADP-ribosyl intermediate by water is a relatively slow process as opposed to the kinetically favored cyclization step (k_3).

The magnitude of the methanolysis/hydrolysis ration in relation to the stabilization of the oxocarbenium ion inter-

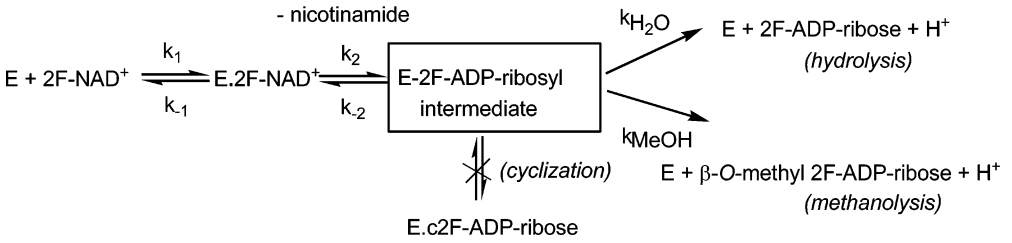

FIGURE 7: Reaction scheme of the transformation of 2-fluoro-NAD+ by *A. californica* ADP-ribosyl cyclase.

mediates has been addressed by one of us for NAD+ glycohydrolase catalyzed reactions (*33*). For *A. californica* ADP-ribosyl cyclase it might however be too simplistic to ascribe the partitioning ratio merely to the relative difference in nucleophilicity of water vs methanol. Indeed, previous work has raised the issue that water accessibility to the active site of such cyclases is likely to be important in determining the fate of the reaction intermediate and controlling the overall balance between hydrolysis and cyclization (*34*). Thus, despite the fact that we observe that solvolysis is proportional to [methanol] between 0 and 3 M, indicating that there is no obvious binding of methanol in this concentration range, we cannot formally exclude the possibility that the *Aplysia* cyclase active site excludes water from the vicinity of the ADP-ribosyl intermediate and that this more "hydrophobic" surrounding may be more favorable to methanol than to water.

It has been reported that, when incubated with *Aplysia* cyclase, NAD+ forms either an oxocarbenium ion intermediate stabilized by an ion pair (*33*) with the "catalytic residue" Glu179 or a covalent acylal intermediate (*21*, *35*) linking the C1″ of the nicotinamide bearing ribose with the same residue. Also, recent crystallographic reports on CD38 seem to advocate the occurrence of a noncovalent intermediate for this protein, although no direct evidence has yet been provided for this (*36*, *37*). While there is evidence to support both such intermediates (*19*), a thorough debate of the advantages of these intermediates is beyond the scope of this work. We adopt here the covalent intermediate model just to describe the reaction pathways involved in the transformation of 2-fluoro-NAD+ catalyzed by *A. californica* ADP-ribosyl cyclase (Figure 8). In the enzyme−substrate intermediate, residues Glu98 and Trp140 of the *Aplysia* cyclase probably position the purine group into a proper conformation (*21*) facilitating nucleophilic attack on the Glu179 bearing carbon (Figure 8). Glu98, as a strong hydrogen bond acceptor, is also found to be a part of the nicotinamide-binding site and is thought to help to stabilize the nicotinamide elimination from the carbon atom linking to Glu179 (*21*).

Thus, we postulate that, when incubated with the *Aplysia* cyclase, 2-fluoro-NAD+ forms an 2-fluoro-ADP-ribosyl intermediate with the Glu179 residue of the enzyme like a normal substrate (see Figure 8). From this intermediate, N1 cyclization leading to the 2-fluoro-cADP-ribose (**7**) is now not possible, although the substrate is presumably aligned in a hairpin conformation, which moves the purine to an appropriate position to accomplish the nucleophilic attack. N7 cyclization, as seen for NHD+ and NGD+, is also unlikely to happen; this has never been observed before for NAD+ or an adenine derivative as these adenosine derivatives, including 2-fluoro-NAD+, are likely to adopt a *syn* conformation in the enzyme−substrate complex and disable any N7 cyclization. 1,N6-Etheno-NAD+ is a known exception that is cyclized enzymatically at the N7 position of the 1,*N*6-ethenoadenine ring. However, since the enzymatic cyclization (unlike chemical cyclization) does not occur at its most nucleophilic etheno N6 position (*38*, *39*), we assume that the 1,N6-etheno-NAD+, in contrast to other adenosine derivatives, may be arranged by the *Aplysia* ADP-ribosyl cyclase in an *anti* conformation due to the presence of the rigid and bulky etheno ring. In agreement with our proposal, the conformational difference was also observed by Yamamoto-Katayama et al. (*40*) when cocrystallizing 1,*N*6-etheno-NAD+ and ATP with CD157 (BST-1). Since a more nucleophilic N7 has been proposed in the case of NGD+ and NHD+ (*41*, *42*), we assume that the etheno ring of 1,*N*6-etheno-NAD+ may also increase the nucleophicility of the N7 position by donating the electron density via the conjugated system, thus also facilitating N7 cyclization. In contrast, the nucleophilicility of N7 in NAD+ is expected to be very low (pK_a of 5′-AMP is −1.6) (*31*) and should be lower in 2-fluoro-NAD+ due to the electron-withdrawing effect of the fluorine group. With the above arguments, we conclude that 2-fluoro-NAD+, like the natural substrate NAD+, is not likely to undergo *Aplysia* cyclase-mediated cyclization at N7. The possibility that 2-fluoro-NAD+ may first be cyclized to the N7-2-fluoro-cADP-ribose (**14**) (Figure 9), since the N1 product is blocked, that is then subsequently very rapidly hydrolyzed to (**5**) is therefore highly unlikely.

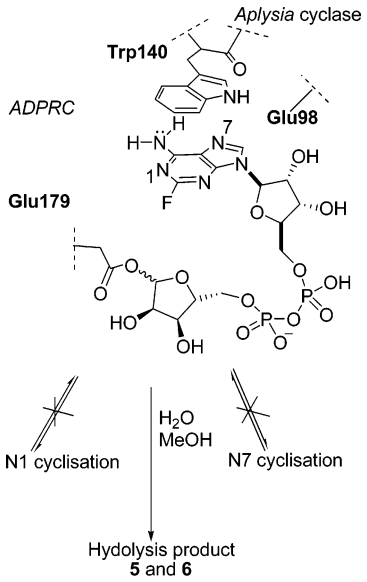

FIGURE 8: Schematic mechanism of 2-fluoro-NAD+/ADP-ribosyl cyclase (ADPRC) interactions, adapted from a previous publication (*30*) based on the binding study (*21*) and the partitioning theory (*17*). The covalent linkage to Glu179 is not proven.

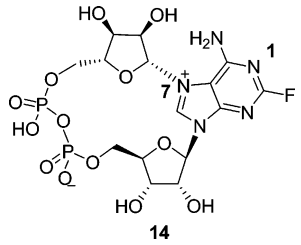

FIGURE 9: Structure of putative N^7-2-fluoro-cADP-ribose.

CONCLUSIONS

We have synthesized 2-fluoro-NAD^+ as a close analogue of NAD^+ and verified the partitioning pathway for *A. californica* ADP-ribosyl cyclase. Incubating 2-fluoro-NAD^+ with ADP-ribosyl cyclase produced a single compound, which was shown to be 2-fluoro-ADP ribose, demonstrating that a NAD^+ glycohydrolase pathway in the partitioning mechanism holds for the *Aplysia* enzyme, since formation of 2-fluoro-cADP-ribose is impossible and a sequential route through the cADP-ribose analogue is not applicable in this case. This was further demonstrated by the methanolysis of 2-fluoro-NAD^+ from which β-1″-*O*-methyl 2-fluoro-ADP-ribose was produced. We conclude, therefore, that 2-fluoro-NAD^+, by allowing the manipulation of some key steps in the kinetic scheme, unmasks the "classical" NAD^+ glycohydrolase function in the *Aplysia* cyclase that remains cryptic with NAD^+ and analogues that can undergo cyclization. Altogether, although *A. californica* ADP-ribosyl cyclase exhibits biological functions different from that of CD38, it can indeed be classified as a multifunctional enzyme even though this is normally masked by the kinetically favored cyclase function.

ACKNOWLEDGMENT

We thank Dr. Andrew Smith for help in molecular modeling and Dr. Christelle Moreau and Dr. Gerd K. Wagner for advice on this paper.

REFERENCES

1. Clapper, D. L., Walseth, T. F., Dargie, P. J., and Lee, H. C. (1987) Pyridine nucleotide metabolites stimulate calcium release from sea urchin egg microsomes desensitized to inositol trisphosphate, *J. Biol. Chem. 262*, 9561−9568.
2. Koshiyama, H., Lee, H. C., and Tashjian, A. H. (1991) Novel mechanism of intracellular calcium release in pituitary cells, *J. Biol. Chem. 266*, 16985−16988.
3. Dargie, P. J., Agre, M. C., and Lee, H. C. (1990) Comparison of Ca^{2+} mobilizing activities of cyclic ADP-ribose and inositol trisphosphate, *Cell Regul. 1*, 279−290.
4. Guse, A. H. (2005) Second messenger function and the structure−activity relationship of cyclic adenosine diphosphoribose (cADPR), *FEBS J. 272*, 4590−4597.
5. Guse, A. H. (2004) Biochemistry, biology, and pharmacology of cyclic adenosine diphosphoribose (cADPR), *Curr. Med. Chem. 11*, 847−855.
6. Lee, H. C., Aarhus, R., and Levitt, D. (1994) The crystal-structure of cyclic ADP-ribose, *Nat. Struct. Biol. 1*, 143−144.
7. Hellmich, M. R., and Strumwasser, F. (1991) Purification and characterization of a molluscan egg-specific NADase, a second-messenger enzyme, *Cell Regul. 2*, 193−202.
8. Lee, H. C., and Aarhus, R. (1991) ADP-ribosyl cyclase: an enzyme that cyclizes NAD^+ into a calcium-mobilizing metabolite, *Cell Regul. 2*, 203−209.
9. Prasad, G. S., McRee, D. E., Stura, E. A., Levitt, D. G., Lee, H. C., and Stout, C. D. (1996) Crystal structure of *Aplysia* ADP ribosyl cyclase, a homologue of the bifunctional ectozyme CD38, *Nat. Struct. Biol. 3*, 957−964.
10. Cakir-Kiefer, C., Muller-Steffner, H., and Schuber, F. (2000) Unifying mechanism for *Aplysia* ADP-ribosyl cyclase and CD38/NAD^+glycohydrolases, *Biochem. J. 349*, 203−210.
11. Howard, M., Grimaldi, J. C., Bazan, J. F., Lund, F. E., Santos-Argumedo, L., Parkhouse, R. M. E., Walseth, T. F., and Lee, H. C. (1993) Formation and hydrolysis of cyclic ADP ribose catalyzed by lymphocyte antigen-CD38, *Science 262*, 1056−1059.
12. Kim, H., Jacobson, E. L., and Jacobson, M. K. (1993) Synthesis and degradation of cyclic ADP ribose by NAD^+glycohydrolases, *Science 261*, 1330−1333.
13. Berthelier, V., Tixier, J. M., Muller-Steffner, H., Schuber, F., and Deterre, P. (1998) Human CD38 is an authentic $NAD(P)^+$ glycohydrolase, *Biochem. J. 330*, 1383−1390.
14. Augustin, A., Muller-Steffner, H., and Schuber, F. (2000) Molecular cloning and functional expression of bovine spleen ecto-NAD^+ glycohydrolase: structural identity with human CD38, *Biochem. J. 345*, 43−52.
15. Muller-Steffner, H., Muzard, M., Oppenheimer, N., and Schuber, F. (1994) Mechanistic implications of cyclic ADP-ribose hydrolysis and methanolysis catalyzed by calf spleen NAD^+glycohydrolase, *Biochem. Biophys. Res. Commun. 204*, 1279−1285.
16. Pacaud, K., Tritsch, D., Burger, A., and Biellmann, J. (2003) Determination of the transglycosidation activity of NAD^+-glycohydrolases with 4-(2′-alkyl-sulfanyl-vinyl)-pyridine derivatives generating chromophoric NAD^+ analogues, *Bioorg. Chem. 31*, 288−305.
17. Muller-Steffner, H. M., Augustin, A., and Schuber, F. (1996) Mechanism of cyclization of pyridine nucleotides by bovine spleen NAD^+glycohydrolase, *J. Biol. Chem. 271*, 23967−23972.
18. Sauve, A. A., Munshi, C., Lee, H. C., and Schramm, V. L. (1998) The reaction mechanism for CD38. A single intermediate is responsible for cyclization, hydrolysis, and base-exchange chemistries, *Biochemistry 37*, 13239−13249.
19. Schuber, F., and Lund, F. E. (2004) Structure and enzymology of ADP-ribosyl cyclases: Conserved enzymes that produce multiple calcium mobilizing metabolites, *Curr. Mol. Med. 4*, 249−261.
20. Cakir-Kiefer, C., Muller-Steffner, H., Oppenheimer, N., and Schuber, F. (2001) Kinetic competence of the cADP-ribose-CD38 complex as an intermediate in the CD38/NAD^+ glycohydrolase-catalyzed reactions: implication for CD38 signalling, *Biochem. J. 358*, 399−406.
21. Love, M. L., Szebenyi, D. M. E., Kriksunov, I. A., Thiel, D. J., Munshi, C., Graeff, R., Lee, H. C., and Hao, Q. (2004) ADP-ribosyl cyclase: Crystal structures reveal a covalent intermediate, *Structure 12*, 477−486.
22. Krolikiewicz, K., and Vorbrüggen, H. (1994) The synthesis of 2-fluoropurine nucleotides, *Nucleosides Nucleotides 13*, 673−678.
23. Montgomery, J. A., and Hewson, K. (1957) Synthesis of potential anticancer agents. X. 2-fluoroadenosine, *J. Am. Chem. Soc. 79*, 4559−4559.
24. Lee, J., Churchill, H., Choi, W., Lynch, J. F., Roberts, F. E., Volante, R. P., and Reider, P. J. (1999) A chemical synthesis of nicotinamide adenine dinucleotide (NAD^+), *Chem. Commun.*, 729−730.
25. Fathi, R., Goswami, B., Kung, P. P., Gaffney, B. L., and Jones, R. A. (1990) Synthesis of 6-substituted 2′-deoxyguanosine derivatives using trifluoroacetic anhydride in pyridine, *Tetrahedron Lett. 31*, 319−322.
26. Gao, H., Fathi, R., Gaffney, B. L., Goswami, B., Kung, P. P., Rhee, Y., Jin, R., and Jones, R. A. (1992) 6-*O*-(Pentafluorophenyl)-2′-deoxyguanosine: a versatile synthon for nucleoside and oligonucleotide synthesis, *J. Org. Chem. 57*, 6954−6959.
27. Kemp, W. (1986) *NMR in Chemistry: A Multinuclear Introduction*, 1st ed., pp 102−107, Macmillan Education Ltd., London.
28. Ikemoto, T., Haze, A., Hatano, H., Kitamoto, Y., Ishida, M., and Nara, K. (1995) Phosphorylation of nucleosides with phosphorus oxychloride in trialkyl phosphate, *Chem. Pharm. Bull. 43*, 210−215.
29. Mukaiyama, T., Matsueda, R., and Suzuki, M. (1970) Peptide synthesis via the oxidation-reduction condensation by the use of 2,2′-dipyridyldisulfide as an oxidant, *Tetrahedron Lett. 11*, 1901−1904.
30. Wagner, G. K., Guse, A. H., and Potter, B. V. L. (2005) Rapid synthetic route toward structurally modified derivatives of cyclic adenosine 5′-diphosphate ribose, *J. Org. Chem. 70*, 4810−4819.
31. Major, D. T., Laxer, A., and Fischer, B. (2002) Protonation studies of modified adenine and adenine nucleotides by theoretical calculations and ^{15}N NMR, *J. Org. Chem. 67*, 790−802.

32. Büchner, P., Maurer, W., and Rüterjans, H. (1978) Nitrogen-15 nuclear magnetic resonance spectroscopy of ^{15}N-labeled nucleotides, *J. Magn. Reson. 29*, 45−63.
33. Tarnus, C., Muller, H. M., and Schuber, F. (1988) Chemical evidence in favor of a stabilized oxocarbonium-ion intermediate in the NAD$^+$ glycohydrolase-catalyzed reactions, *Bioorg. Chem. 16*, 38−51.
34. Munshi, C., Thiel, D. J., Mathews, I. J., Aarhus, R., Walseth, T. F., Lee, H. C. (1999) Characterization of the active site of ADP-ribosyl cyclase, *J. Biol. Chem. 274*, 30770−30777.
35. Sauve, A. A., Deng, H. T., Angeletti, R. H., and Schramm, V. L. (2000) A covalent intermediate in CD38 is responsible for ADP-ribosylation and cyclization reactions, *J. Am. Chem. Soc. 122*, 7855−7859.
36. Liu, Q., Kriksunov, I. A., Graeff, R., Lee, H. C., and Hao, Q. (2006) Structural basis for the mechanistic understanding of human CD38-controlled multiple catalysis, *J. Biol. Chem. 281*, 32861−32869.
37. Liu, Q., Kriksunov, I. A., Graeff, R., Lee, H. C., and Hao, Q. (2007) Structural basis for formation and hydrolysis of the calcium messenger cyclic ADP-ribose by human CD38, *J. Biol. Chem. 282*, 5853−5861.
38. Guengerich, F. P., and Raney, V. M. (1992) Formation of etheno adducts of adenosine and cytidine from 1-halooxiranes. Evidence for a mechanism involving initial reaction with the endocyclic nitrogen atoms, *J. Am. Chem. Soc. 114*, 1074−1080.
39. Zhang, F.-J., and Sih, C. J. (1995) Enzymatic cyclization of 1,N^6-etheno-nicotinamide adenine dinucleotide, *Bioorg. Med. Chem. Lett. 5*, 1701−1706.
40. Yamamoto-Katayama, S., Ariyoshi, M., Ishihara, K., Hirano, T., Jingami, H., and Morikawa, K. (2002) Crystallographic studies on human BST-1/CD157 with ADP-ribosyl cyclase and NAD$^+$ glycohydrolase activities, *J. Mol. Biol. 316*, 711−723.
41. Zhang, F. J., and Sih, C. J. (1995) Novel enzymatic cyclizations of pyridine nucleotide analogues: cyclic-GDP-ribose and cyclic-HDP-ribose, *Tetrahedron Lett. 36*, 9289−9292.
42. Potter, B. V. L., and Walseth, T. F. (2004) Medicinal chemistry and pharmacology of cyclic ADP-ribose, *Curr. Mol. Med. 4*, 303−311.

BI061933W